

# Characterisation of the solid solution $\text{La}(\text{Ni},\text{Fe})\text{O}_3$ prepared via a sol-gel related method using propionic acid

H. PROVENDIER, C. PETIT, J.-L. SCHMITT, A. KIENNEMANN  
*Laboratoire d'Etude de la Réactivité Catalytique, des Surfaces et des Interfaces- ECPM, UMR 7515-25, rue Becquerel 67035, Strasbourg, Cedex, France*  
E-mail: kiennemann@chimie.u-strasbg.fr

C. CHAUMONT  
*Groupe des Matériaux Inorganiques, ECPM, 23, rue du Loess 67037, Strasbourg, Cedex, France*

The paper shows the possible obtaining of the solid solution of  $\text{LaNiO}_3$  and  $\text{LaFeO}_3$  by a sol-gel like method with propionate acid as solvent. In order to understand the role of the precursor nature in function of the starting materials on the formation or not of  $\text{LaNi}_x\text{Fe}_{1-x}\text{O}_3$ , an identification using infrared spectroscopy was made. The solid solution formation needs the limitation of the preferential  $\text{LaFeO}_3$  in order to permit the introduction of nickel into the structure. Nitrate salts of iron and lanthanum gave pure  $\text{LaNi}_x\text{Fe}_{1-x}\text{O}_3$  perovskite with a high homogeneity even at nanoscopic scale. © 1999 Kluwer Academic Publishers

## 1. Introduction

Natural gas is a particular abundant, clean and easily extractable energy source [1]. Unfortunately its production sites are located far away from the exploitation sites and its transport remains expensive and dangerous [2, 3]. It is thus of interest to convert it into liquid fuel via an intermediate mixture of  $\text{CO}$ ,  $\text{CO}_2$  and  $\text{H}_2$ , called synthesis gas [4]. The transformation occurs mainly via a catalytic way by addition to natural gas of an oxidant, which is often water [5], but which can also be oxygen or carbon dioxide [6, 7]. The catalysts containing nickel are the most used because of their fast turnover rate, cost and long term stability [8]. The catalytic reaction is performed at high temperature ( $800^\circ\text{C}$ ) and metal nickel is the active species [9]. However, nickel tends to sinter [10] in the reaction conditions, which leads to diminish the number of active sites and to increase the carbon deposition.

The initial interaction of nickel with the support under the form of an aluminate ( $\text{NiAl}_2\text{O}_4$ ) [11] or a lanthanate ( $\text{LaNiO}_3$ ) [12] is considered favourable to the good working of the catalyst, because it can limit the sintering of metal particles by the interaction between Ni and the support [13]. So, the initial formation of a definite structure represents a new and interesting route in the catalysis of synthesis gas production [6]. Perovskite structures are widely studied for their intrinsic properties [14] and their applications in electrochemistry, supraconductivity [15] and especially in catalysis [16]. It has been shown, that the combination of nickel with a second element of the VIII group into a lanthanum perovskite structure  $\text{La}(\text{Ni}, \text{M})\text{O}_3$  presented

interesting properties in catalysis like the preserving of a perovskite phase during reaction and a strong interaction between nickel and the structure, limiting metal crystallite growth and carbon deposition [17]. Especially iron is interesting because of its stabilising effect on the structure [18]. The ionic radii of Fe (+III) and Ni (+III) are of similar size order, which permits to afford the formation of a  $\text{LaNiO}_3$ - $\text{LaFeO}_3$  solid solution [19, 20]. Moreover both  $\text{LaFeO}_3$  [21] and  $\text{LaNiO}_3$  [22] perovskite structures exist and they present cubic perovskite structures with orthorhombic and rhomboedral distortions respectively.

In this paper different preparations either via a ceramic method using oxides or via a sol-gel related method using propionic acid as solvent and various starting materials (nitrate, acetate, oxide, metal) were studied for the formation of  $\text{LaNi}_{0.3}\text{Fe}_{0.7}\text{O}_3$ .

Only few of them lead to the obtaining of the solid solution. The conditions required for its formation are linked to the preparation method and to the nature of the starting materials. In the appropriate conditions, all products of the solid solution  $\text{LaNi}_x\text{Fe}_{1-x}\text{O}_3$  ( $0 \leq x \leq 1$ ) with a step of 0.1 could be prepared and studied.

## 2. Experimental

### 2.1. Choice of the preparation method and of the starting materials

A preparation was carried out via a ceramic method starting from oxides: the oxides were mixed, crushed together, pressed into 200 mg pellets and calcined at

TABLE I Characteristic peaks of mono and bidentate propionates and of nitrates

IR peaks ( $\text{cm}^{-1}$ ) products	$\nu\text{sCO}$	$\nu\text{sCOO}$	$\delta\text{asCH}_3$	$\nu\text{sCOO}$	$\delta\text{sCH}_3$ and $\nu_3 \text{NO}$	$\nu\text{sCH}_2$	$\nu_2 \text{NO}$
Monodentate propionate		1570		1410			
Bidentate propionate		1520		1420			
Propionic acid	1710		1468		1380	1332	
Nitrates					1380		830

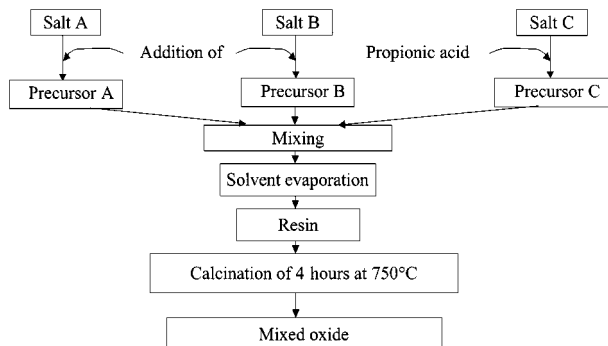


Figure 1 Scheme of preparation via a sol-gel related method.

750 °C. This treatment was performed three times in order to get a better homogeneity of the system.

All other preparations follow a sol-gel related method using propionic acid as solvent [23] and described in Fig. 1.

Before use, lanthanum oxide was calcined 12 h at 900 °C in order to decompose the easily formed lanthanum hydroxides, which would lead to a stoichiometry defect in the final product. This method requires the preliminary formation of clear La, Ni and Fe solutions, obtained after total dissolution of the starting materials in propionic acid. After dissolution, the Ni and Fe solutions were mixed and added to the La solution. After a 30 min stirring, the solvent was evaporated until the formation of a resin or a foam, which was calcined under a temperature increase with a slope of 3 °C · min<sup>-1</sup> from 25–750 °C and maintained 4 h at 750 °C. The critical point of this method, especially observed in large scale preparations, is the evaporation of the solvent, which sometimes leads to the decomposition of nitrates with violent NO<sub>2</sub> production. So, a slow and controlled distillation is recommended for this step. Even prepared in small amounts, the resin tends to become red with incandescent points and finally burns to a black powder.

In order to avoid or limit this phenomenon, other starting materials as nitrates have to be tested for the preparation of the solid solution. The differences observed at the end of the evaporation of the solvent depending on the starting materials must be linked to the state of the precursors in the solutions.

## 2.2. Obtention of the precursors and oxides

Therefore a study on the formation of the precursors observed in the propionic acid solution, depending on the starting materials used, was carried out following a method developed by Roger [24]. In this method, the solution obtained by dissolution of a starting material into propionic acid is concentrated by a partial evaporation of the solvent. Hexane is added as counter-solvent

to this solution until the appearance of a white precipitate. Then this mixture is kept in the freezer at –10 °C until the formation of crystals. The obtained crystals are rapidly filtered, washed with hexane and analysed by FT-IR in a KBr matrix containing 3 wt % of product. The FT-IR spectra were obtained on a Nicolet 5DXC spectrometer with Fourier transform. The characteristic peaks for mono- or bidentate propionates [24, 25], propionic acid and nitrates are given in Table I.

After calcination the final products were characterised by X-Ray Diffraction (XRD) on a Siemens D5000TT diffractometer using CuK<sub>α</sub> radiation, by Scanning Electron Microscopy (SEM) on a JEOL JSM 840 microscope, by elemental analysis performed in the CNRS Centre in Vernaison and by specific surface measurements (BET).

Depending on the starting materials and the former precursors the LaNi<sub>x</sub>Fe<sub>1-x</sub>O<sub>3</sub> solid solution was obtained or not. In the case of its formation, the products were characterised by Transmission Electron Microscopy (TEM) on a Topcon EM 002B microscope (accelerating voltage of 200 kV) coupled to an Energy Dispersive X-ray Spectroscopy (EDS).

## 3. Results and discussion

### 3.1. Characterization of the precursors

Using the ceramic preparation method, the LaNi<sub>x</sub>Fe<sub>1-x</sub>O<sub>3</sub> solid solution was not obtained but a mixture of LaNiO<sub>3</sub>, LaFeO<sub>3</sub> and of the starting oxides NiO, La<sub>2</sub>O<sub>3</sub> and Fe<sub>2</sub>O<sub>3</sub> was observed. This was quite expectable because this method requires a much higher calcination temperature (1200 °C) in order to have a sufficient diffusion of the elements. However, in our case, the temperature is limited by the transformation of LaNiO<sub>3</sub> into La<sub>2</sub>NiO<sub>4</sub> and NiO above 860 °C. As shown previously [26] the common used method is a sol-gel related method. This method was tested using various starting materials (either nitrates, acetates, oxides or metals of La, Ni and Fe). However, only those, which were totally soluble in propionic acid were kept for the preparation. The study of the redox potential is a good indicator of the solubility of metallic elements [27]. Whereas metallic iron easily dissolved in hot propionic acid, metallic nickel was not soluble even after two days. Nitrate and oxide were retained for La, nitrate and metallic iron for Fe and nitrate and acetate for Ni. The different possible combinations of starting materials for the LaNi<sub>x</sub>Fe<sub>1-x</sub>O<sub>3</sub> preparation are given in Table II.

In order to test the influence of the starting material nature and to choose the most appropriate combination for the preparation, a study of the precursors was performed.

TABLE II Combinations of starting materials tested for the preparation of the  $\text{LaNi}_x\text{Fe}_{1-x}\text{O}_3$  solid solution

No.	Starting material (La)	Starting material (Fe)	Starting material (Ni)
1	Nitrate $\text{La}(\text{NO}_3)_3, 6\text{H}_2\text{O}$	Nitrate $\text{Fe}(\text{NO}_3)_3, 9\text{H}_2\text{O}$	Nitrate $\text{Ni}(\text{NO}_3)_2, 6\text{H}_2\text{O}$
2	Nitrate $\text{La}(\text{NO}_3)_3, 6\text{H}_2\text{O}$	Nitrate $\text{Fe}(\text{NO}_3)_3, 9\text{H}_2\text{O}$	Acetate $\text{Ni}(\text{C}_2\text{H}_3\text{O}_2)_2, 6\text{H}_2\text{O}$
3	Nitrate $\text{La}(\text{NO}_3)_3, 6\text{H}_2\text{O}$	Metal Fe	Nitrate $\text{Ni}(\text{NO}_3)_2, 6\text{H}_2\text{O}$
4	Nitrate $\text{La}(\text{NO}_3)_3, 6\text{H}_2\text{O}$	Metal Fe	Acetate $\text{Ni}(\text{C}_2\text{H}_3\text{O}_2)_2, 6\text{H}_2\text{O}$
5	Oxide $\text{La}_2\text{O}_3$	Nitrate $\text{Fe}(\text{NO}_3)_3, 9\text{H}_2\text{O}$	Nitrate $\text{Ni}(\text{NO}_3)_2, 6\text{H}_2\text{O}$
6	Oxide $\text{La}_2\text{O}_3$	Nitrate $\text{Fe}(\text{NO}_3)_3, 9\text{H}_2\text{O}$	Acetate $\text{Ni}(\text{C}_2\text{H}_3\text{O}_2)_2, 6\text{H}_2\text{O}$
7	Oxide $\text{La}_2\text{O}_3$	Metal Fe	Nitrate $\text{Ni}(\text{NO}_3)_2, 6\text{H}_2\text{O}$
8	Oxide $\text{La}_2\text{O}_3$	Metal Fe	Acetate $\text{Ni}(\text{C}_2\text{H}_3\text{O}_2)_2, 6\text{H}_2\text{O}$

TABLE III IR peaks ( $\text{cm}^{-1}$ ) of the precursors depending on the starting materials

IR peaks ( $\text{cm}^{-1}$ ) starting materials	$\nu\text{sCO}$	$\nu\text{asCOO}$	$\delta\text{asCH}_3$	$\nu\text{sCOO}$	$\nu\text{NO}_3$	$\delta\text{sCH}_3$	$\nu\text{sCH}_2$	$\nu\text{NO}_3$
Lanthanum nitrate		1522	1469	1435	1384		1296	825
Lanthanum oxide	1716	1560	1468	1433		1378	1296	
Iron nitrate		1574	1468	1434	1380		1304	825
Metallic iron		1573	1468	1430		1375	1302	
Nickel nitrate		1570	1467	1414	1384		1302	825
Nickel acetate		1570	1467	1415		1377	1300	

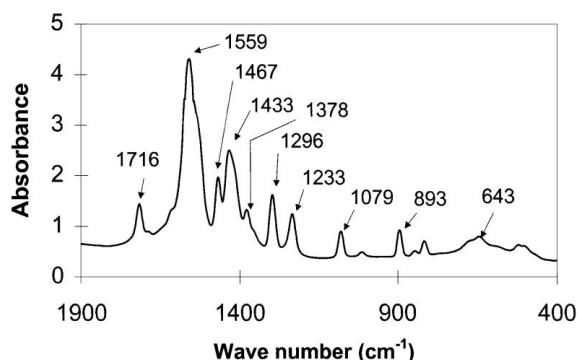
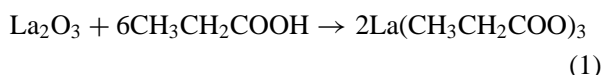


Figure 2 FTIR of precursor made from lanthanum oxide in propionic acid (monodentate La propionate).

Crystals were obtained from the solutions of starting materials dissolved in propionic acid, following the method described in the experimental part. The IR spectra of these crystals indicate the nature of the precursors of each element used for the preparation of the perovskite structure. The IR peaks observed for these starting material precursors are given in Table III. The IR study of the crystals obtained from the metallic iron solution has shown the formation of a monodentate lanthanum propionate (Fig. 2).

This formation results from the oxido-reduction reaction (1):



For the nickel acetate and for the iron solutions in propionic acid, propionates have also been observed. In these cases, nickel and lanthanum remained at the valence states +2 and +3 respectively, like in the starting materials used, whereas  $\text{Fe}^\circ$  is oxidised into  $\text{Fe}(+\text{III})$ .

However, starting from nitrate salts, the propionate to nitrate substitution seems to be more difficult. This substitution depends on the nature of the element and on its hydration rate as shown Table IV. Indeed, as a

TABLE IV Nature of the precursors in propionic acid versus the starting materials

Element	Starting material	Precursors in propionic acid
La	Lanthanum nitrate	Nitrates + few bidentate propionates
La	Lanthanum oxide	Monodentate propionates
Fe	Iron nitrate	Nitrates + few monodentate propionates
Fe	Metallic iron	Monodentate propionates
Ni	Nickel nitrate	Nitrates + few monodentate propionates
Ni	Nickel acetate	Monodentate propionates

first step, the presence of water in the starting materials helps the nitrate salts to dissolve in propionic acid in creating a separation between the metallic cation and the nitrate anions. The solvolysis occurs slowly for the three elements and if the solvent is evaporated rapidly a foam formation corresponding to nitrate departure can be observed for Ni and Fe solutions. A slow evaporation of the solvent leads progressively to the total nitrate departure and to the propionate formation, but in this case, the particular interest of the various nature of the starting material disappears. So a fast evaporation of the solvent was chosen for this study and for the preparation of the perovskite structure. This explains why nitrate and propionate peaks coexist in the IR spectra for the three nitrate salts of La, Ni and Fe. In the case of lanthanum nitrate, the IR spectra showed a intense nitrate peak, indicating that the substitution of nitrate by propionate is more difficult than for Ni and Fe. Table IV gathers the nature of the precursors observed in the propionic acid solution depending on the starting materials used.

Using all the possible combinations of these starting materials, eight preparations of the  $\text{LaNi}_{0.3}\text{Fe}_{0.7}\text{O}_3$  structure were tested and characterised by X-ray diffraction. XRD detected phases are given versus the starting materials used in Table V. The XRD diagrams

TABLE V XRD detected crystalline phases versus the starting materials used

No.	Starting materials			Propionate formation			Crystalline XRD phases
	La	Fe	Ni	La	Fe	Ni	
1	Nitrate	Nitrate	Nitrate	Few bi	Few Mono	Few Mono	$\text{LaNi}_{0.3}\text{Fe}_{0.7}\text{O}_3$
2	Nitrate	Nitrate	Acetate	Few bi	Few Mono	Mono	$\text{LaNi}_{0.3}\text{Fe}_{0.7}\text{O}_3$
3	Nitrate	Metal	Nitrate	Few bi	Mono	Few Mono	$\text{LaNi}_{0.3}\text{Fe}_{0.7}\text{O}_3$
4	Nitrate	Metal	Acetate	Few bi	Mono	Mono	$\text{LaNi}_{0.3}\text{Fe}_{0.7}\text{O}_3$
5	Oxide	Nitrate	Nitrate	Mono	Few Mono	Few Mono	$\text{LaNi}_{0.2}\text{Fe}_{0.8}\text{O}_3$
6	Oxide	Nitrate	Acetate	Mono	Few Mono	Mono	$\text{LaNi}_{0.2}\text{Fe}_{0.8}\text{O}_3$
7	Oxide	Metal	Nitrate	Mono	Mono	Few Mono	$\text{NiO/La}_2\text{O}_3, \text{LaFeO}_3$
8	Oxide	Metal	Acetate	Mono	Mono	Mono	$\text{NiO/La}_2\text{O}_3, \text{LaFeO}_3$

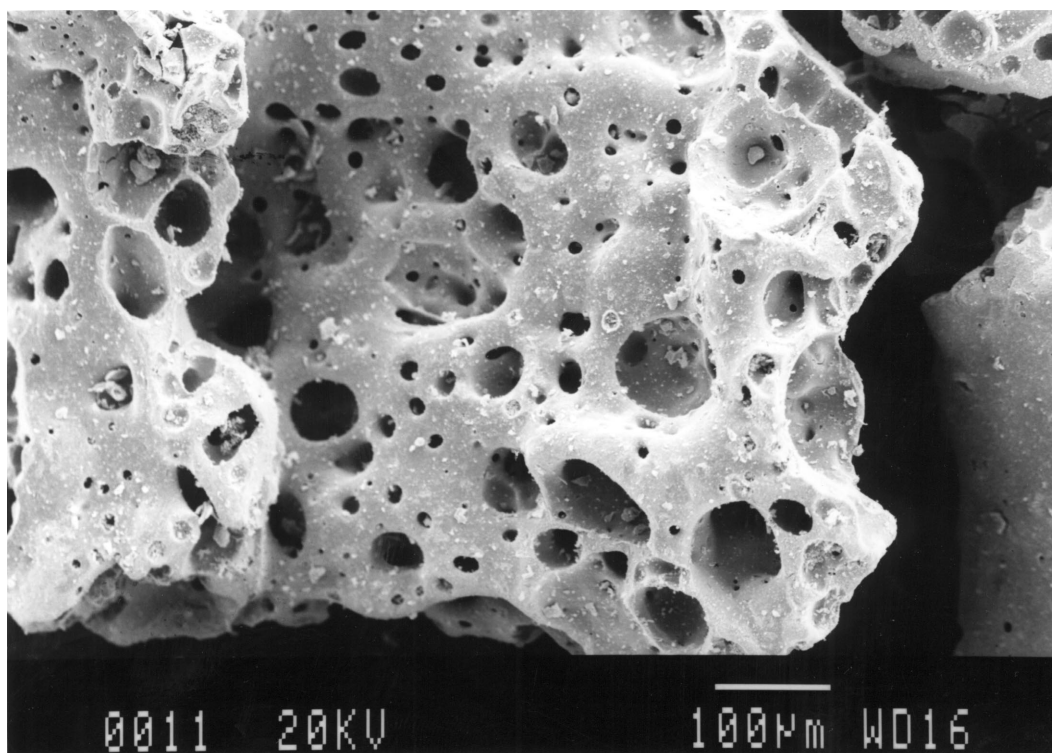


Figure 3 SEM micrograph for the La-Ni-Fe perovskite made with all nitrate salts and Ni/Fe = 0.3/0.7 (sample No. 1).

showed the formation of the desired structure for the combinations Nos. 1 to 4. The presence of an under stoichiometric perovskite structure in nickel was noted for the combinations Nos. 5 and 6 (remaining NiO and  $\text{La}_2\text{O}_3$  could not be detected by XRD), whereas three phases NiO,  $\text{La}_2\text{O}_3$  and  $\text{LaFeO}_3$  were observed for the combinations Nos. 7 and 8.

The results obtained by XRD show clearly that all the preparations using lanthanum nitrate as starting material present the formation of the expected  $\text{LaNi}_{0.3}\text{Fe}_{0.7}\text{O}_3$  structure [26, 28]. This leads to the conclusion that lanthanum nitrate is necessary to the preparation of the  $\text{LaNi}_{0.3}\text{Fe}_{0.7}\text{O}_3$  structure. In the absence of lanthanum nitrate, the nickel is not or partially not inserted in the perovskite structure. This phenomenon can be related to the preferential formation of the stable  $\text{LaFeO}_3$  perovskite structure, resulting in the exclusion of nickel of the structure. Probably the presence of nitrates around the lanthanum ions in the propionic solution limits this preferential  $\text{LaFeO}_3$  formation and permits the insertion of nickel into the structure.

Evident differences have been noticed in the BET specific surface area measurements and on the SEM

micrographs between the bordering preparations No. 1 using only nitrate salts (Fig. 3) and No. 8 using no nitrates (Fig. 4). While the BET value is equal to  $5.8 \text{ g} \cdot \text{m}^{-2}$  for No. 1, it is lowered to  $2.5 \text{ g} \cdot \text{m}^{-2}$  for No. 8. Whereas No. 1 shows holes, corresponding to nitrate departure during the step of evaporation of the solvent, No. 8 presents a smooth surface, which explains the lower BET value and which is unfavourable to a catalytic application.

### 3.2. Preparation of the total solid solution and characterisation

The preparation of all compounds of the  $\text{LaNi}_x\text{Fe}_{1-x}\text{O}_3$  series with  $0 \leq x \leq 1$ , nitrate salts have been chosen as La, Ni and Fe starting materials, following the results of the previous study. The elemental distribution in the  $\text{LaNi}_x\text{Fe}_{1-x}\text{O}_3$  sample series prepared via the sol-gel related method has been determined by elemental analysis in Vernaison and agrees well with the theoretical values (relative errors inferior to 1%). The XRD analysis has shown that in each case only one perovskite phase is obtained (Fig. 5). Moreover, a zoom in the

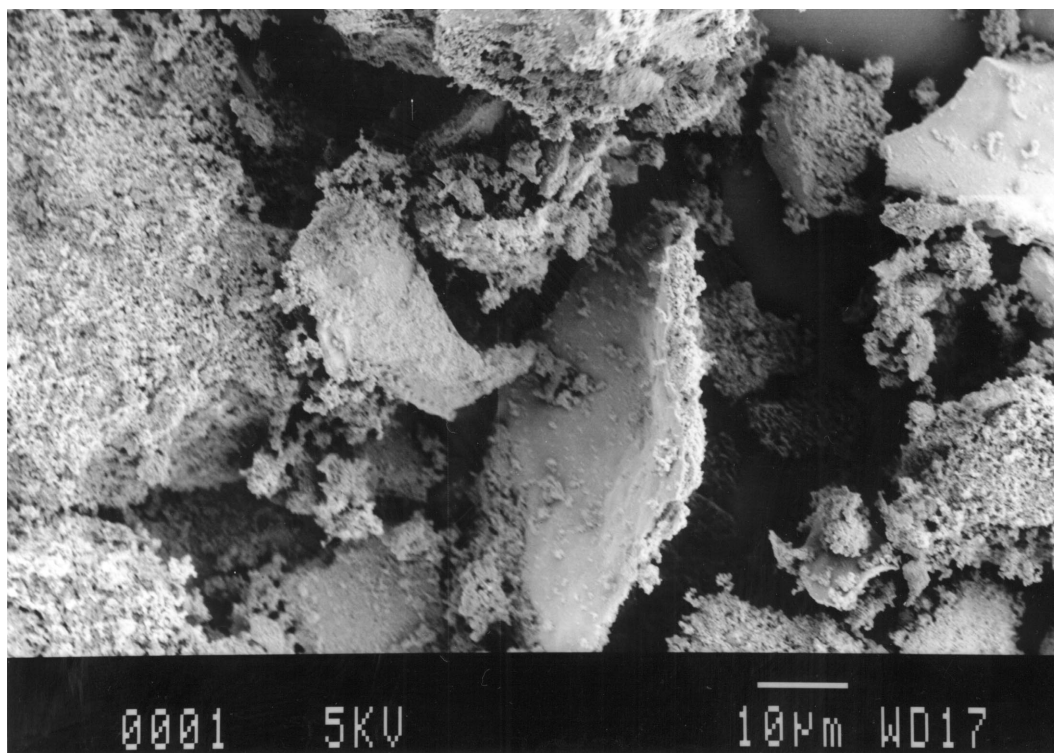


Figure 4 SEM micrograph for the La-Ni-Fe perovskite made without nitrate salts and Ni/Fe = 0.3/0.7 (sample No. 8).

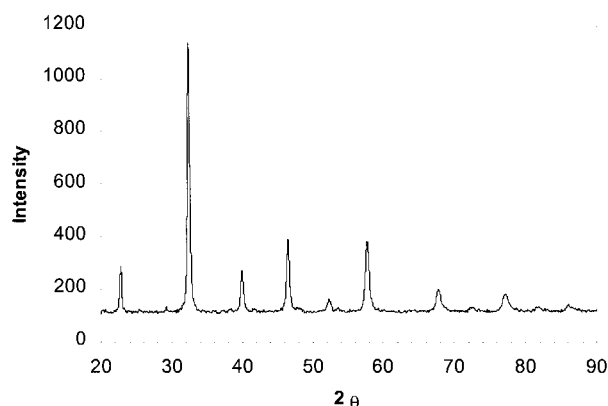


Figure 5 DRX analysis of La-Ni-Fe perovskite made with all nitrate salts and Ni/Fe = 0.3/0.7 (sample No. 1) in the area  $20.0 \leq 2\theta \leq 90.0$  ( $2\theta$ ).

area of the most intensive peak ( $31.5 \leq 2\theta \leq 33.0$ ) presents a progressive and regular shift of the peak positions from  $\text{LaFeO}_3$  to  $\text{LaNiO}_3$  reference phases with increasing  $x$  (Fig. 6). According to the Vegard's law [29] to the formation of the  $\text{LaNi}_x\text{Fe}_{1-x}\text{O}_3$  solid solution for  $0 \leq x \leq 1$  with a 0.1 step was concluded.

The lattice parameter of these structures assimilated pseudo-cubic has been calculated using the six most intensive XRD peaks and reported vs.  $x$  (Fig. 7). The curve obtained is linear and presents lattice parameters of 3.92 and 3.84 Å respectively for  $\text{LaFeO}_3$  and  $\text{LaNiO}_3$  in agreement with the reference values calculated using the JCPDS files, 3.93 and 3.85 Å respectively.

This confirms the formation, by this preparation method, of a  $\text{La}(\text{Ni}, \text{Fe})\text{O}_3$  solid solution, as recently proposed by Garcia *et al.* for a citrate precipitation method [30]. However, in our case, the solid solution

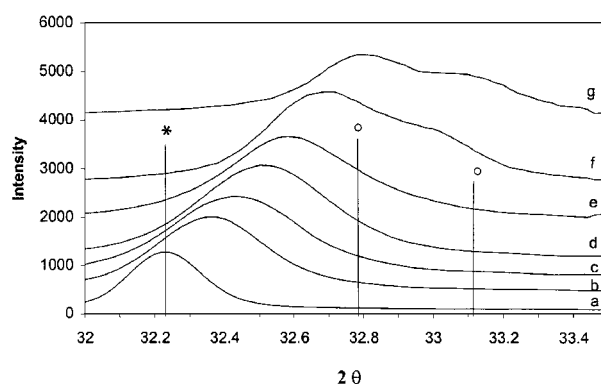


Figure 6 DRX analysis of La-Ni-Fe perovskite made with all nitrate salts and Ni/Fe = 0.3/0.7 (sample No. 1) in the area  $31.5 \leq 2\theta \leq 33.0$  ( $2\theta$ ) with the references \* for  $\text{LaFeO}_3$  and ° for  $\text{LaNiO}_3$ .

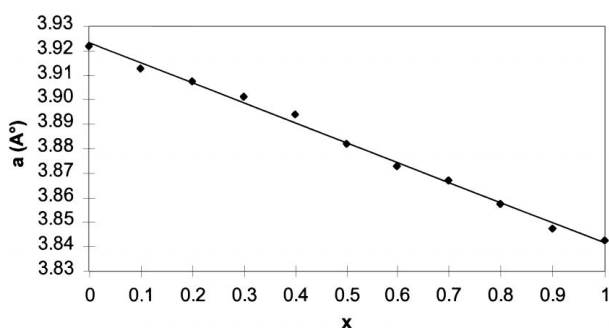


Figure 7 Lattice parameter vs.  $x$  for  $\text{LaNi}_x\text{Fe}_{1-x}\text{O}_3$  solid solution.

is observed in all proportions for  $0 \leq x \leq 1$  inclusive for  $x = 0.5$ . In order to confirm the formation of the solid solution, also at a nanoscopic scale, the homogeneity of the samples has been studied by TEM-EDS. The micrographs show the regular succession of the atomic planes, which can belong to different planes of

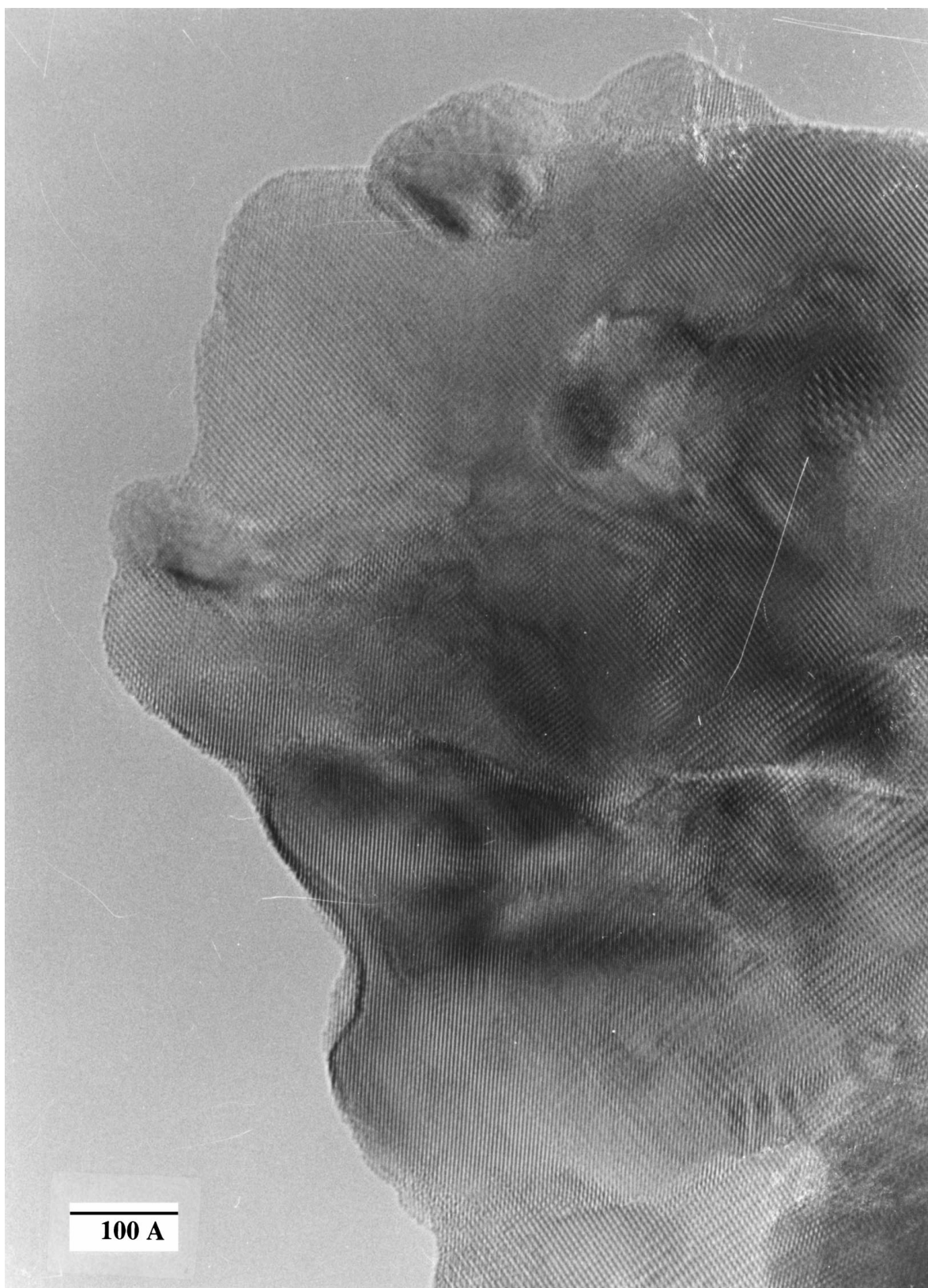


Figure 8 TEM of La-Ni-Fe perovskite made with all nitrate salts and Ni/Fe = 0.3/0.7 (sample No. 1:  $\text{LaNi}_{0.3}\text{Fe}_{0.7}\text{O}_3$ ).

the lattice, as presented for  $\text{LaNi}_{0.3}\text{Fe}_{0.7}\text{O}_3$  (Fig. 8). The interreticular distances measured on these micrographs correspond to those of  $\text{LaNi}_x\text{Fe}_{1-x}\text{O}_3$  perovskite lattice. However, the precision is not sufficient to distinguish differences versus  $x$  and the multiplicity of the observed planes is too high to calibrate them. For these reasons, TEM does not permit to reach the nickel stoichiometry in the solid solution.

EDS measurements have been carried out on different areas of the samples, using either a broad (200 nm diameter) focused beam or using a fine (14 nm diameter) focused beam. As shown by Houalla *et al.* [31], the use of a fine focused beam in the scanning transmission mode for X-Ray microanalyses gives information about the sample homogeneity, whereas the broad focused beam leads to the mean elemental proportions in the

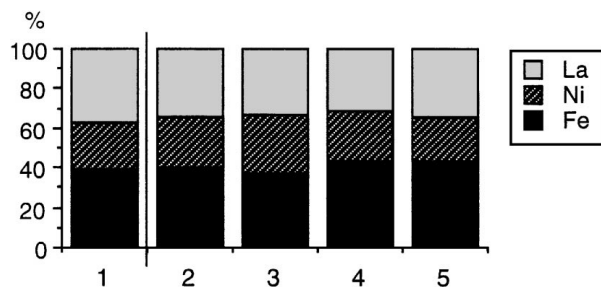


Figure 9 EDS analysis of  $\text{LaNi}_x\text{Fe}_{1-x}\text{O}_3$  with  $x = 0.3$ , No. 1 large focused beam (200 nm), Nos. 2–5 fine focused beam (14 nm).

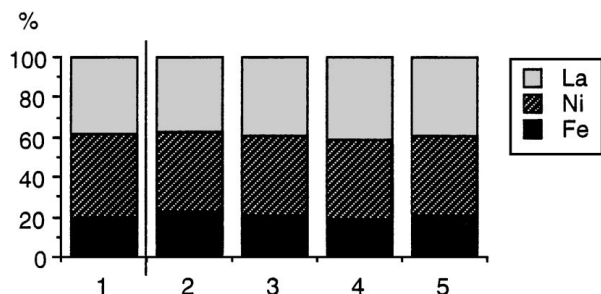


Figure 10 EDS analysis of  $\text{LaNi}_x\text{Fe}_{1-x}\text{O}_3$  with  $x = 0.7$ , No. 1 large focused beam (200 nm), Nos. 2–5 fine focused beam (14 nm).

sample. The two  $\text{LaNi}_{0.3}\text{Fe}_{0.7}\text{O}_3$  and  $\text{LaNi}_{0.7}\text{Fe}_{0.3}\text{O}_3$  systems are presented as examples for the EDS analyses, respectively in Figs 9 and 10 and it is clearly to see that the prepared systems are very homogeneous.

#### 4. Conclusion

A preliminary study on the preparation methods and on the starting materials has permitted to show the influence of the precursors and to select an appropriate way for the formation of the  $\text{LaNi}_x\text{Fe}_{1-x}\text{O}_3$  solid solution. All compounds of this  $\text{LaNi}_x\text{Fe}_{1-x}\text{O}_3$  series, with  $0 \leq x \leq 1$  and a 0.1 step, have been successfully prepared via a sol-gel related method using propionic acid as solvent and nitrate salts as starting materials. The characterisations by XRD and TEM have demonstrated the formation of the La-Ni-Fe solid solution in all proportions and the good homogeneity of the prepared systems has been proved by the constant local elemental distribution given by EDS. These interesting properties are in favour of a catalysis application of these mixed perovskite  $\text{LaNi}_x\text{Fe}_{1-x}\text{O}_3$  systems.

#### References

1. S. FIELD, S. C. NIRULA and J. G. McCARTY, Report from S.R.I. international IV 69129-01-SQ, 1987.
2. J. SAINT-JUST, J. M. BASSET, J. BOUSQUET and G. A. MARTIN, *La Recherche* **222** (1990) 731.

3. R. P. BAUQUIS, *Revue de l'Institut Français du Pétrole* **51** (1996) 615.
4. J. R. ROSTRUP-NIELSEN, *Catal. Today* **18** (1993) 305.
5. *Idem.*, in J. R. ANDERSON and M. BOUDART, "Catalytic Steam Reforming, Catalysis, Science and Technology," Vol. 5, edited by J. R. Anderson and M. Boudart (Springer, Berlin, 1984) p. 1.
6. S. C. TSANG, J. B. CLARIDGE and M. L. H. GREEN, *Catal. Today* **23** (1995) 3.
7. S. B. WANG, G. Q. M. LU and G. J. MILLAR, *Energy and Fuels* **10** (1996) 896.
8. J. DE DEKEN, P. G. MENON, G. F. FROMENT and G. HAEMERS, *J. Catal.* **70** (1981) 225.
9. V. R. CHOUDHARY, V. H. RANE and A. M. RAJPUT, *Catal. Lett.* **22** (1993) 289.
10. V. C. H. KROLL, H. M. SWAAN and C. MIRODATOS *J. Catal.* **161** (1996) 409.
11. D. DISSANAYAKE, M. P. ROSYNEK, KCC. KHARAS and J. H. LUNSFORD, *ibid.* **132** (1991) 117.
12. A. SLAGTERN, U. OLSBYE, R. BLOM, I. M. DAHL and H. FJELLVAG, *Appl. Catal.* **145** (1996) 375.
13. C. PETIT, A. KIENNEMANN, P. CHAUMETTE and O. CLAUSE, US Patent No. 5,447,705 (1995).
14. J. TWU and P. K. GALLAGHER, in "Properties and Application of Perovskite Type Oxides," edited by L. G. Tejuca and J. L. G. Fierro (Marcel Dekker, New York 1993) p. 1.
15. A. K. RAYCHAUDHURI, *Adv. In Phys.* **44** (1995) 21.
16. T. SEIYAMA, in "Properties and Application of Perovskite Type Oxides," edited by L. G. Tejuca and J. L. G. Fierro (Marcel Dekker, New York 1993) p. 215.
17. T. HAYAKAWA, H. HARIHARA, A. G. ANDERSEN, K. SUZUKI, H. YASUDA, T. TSUNODA, S. HAMAKAWA, A. P. E. YORK, Y. S. YOON, M. SHIMIZU and K. TAKEHIRA, *Appl. Catal. A* **149** (1997) 391.
18. H. PROVENDIER, C. PETIT, C. ESTOURNES, S. LIBS and A. KIENNEMANN, *Appl. Catal. A* **180** (1999) 163.
19. H. FALCON, A. E. GOETA, G. PUNTE and R. E. CARBONIO, *J. Solid State Chem.* **133** (1997) 379.
20. N. E. MASSA, H. FALCON, H. SALVA and R. E. CARBONIO, *Phys. Review B, Condensed matter* **56** (1997) 10178.
21. A. GOLUB, L. S. SIDORIK, S. A. MEDICKO and M. FEDORUK, *Inorg. Mater* **14** (1978) 1449.
22. Mc MURDIE, *Powder Diffraction* **1** (1986) 269.
23. J. L. REHSPRINGER and J. C. BERNIER, *Mat. Res. Soc. Symp. Proc.* **72** (1986) 67.
24. A. C. ROGER, C. PETIT and A. KIENNEMANN, *J. Catal.* **167** (1997) 447.
25. M. J. TAYLOR and J. M. CODDINGTON, *Polyhedron* **11** (1992) 1531.
26. H. PROVENDIER, C. PETIT, G. EHRET and A. KIENNEMANN, *J. Chim. Phys IV France* (1998) 8.
27. G. SINQUIN, Thesis, Strasbourg, France 1998.
28. H. PROVENDIER, C. PETIT, A. C. ROGER and A. KIENNEMANN, *Stud. Surf. Sci. Catal.* **118** (1998) 285.
29. A. GUINIER, in "Théorie et technique de la rariocristallographie," edited by Dunod (1964) p. 371.
30. J. GARCIA, J. BLASCO, M. G. PROIETTI, M. BENFATTO, *Phys Review B. Condensed Matter* **52** (1995) 15823.
31. M. HOUALLA, F. DELANNAY, I. MATSUURAI and B. DELMON, *J. C. S. Faraday* **176** (1980) 2128.

Received 9 December 1998  
and accepted 15 March 1999